

Bulk modulus and its pressure derivative of $\text{YBa}_2\text{Cu}_3\text{O}_{7-x}$

M. Cankurtaran and G. A. Saunders

School of Physics, University of Bath, Claverton Down, Bath, BA2 7AY, England

J. R. Willis

School of Mathematical Sciences, University of Bath, Claverton Down, Bath, BA2 7AY, England

A. Al-Kheffaji

School of Physics, University of Bath, Claverton Down, Bath, BA2 7AY, England

D. P. Almond

School of Materials Science, University of Bath, Claverton Down, Bath, BA2 7AY, England

(Received 24 August 1988)

Pressure dependences of the ultrasonic wave velocities in polycrystalline $\text{YBa}_2\text{Cu}_3\text{O}_{7-x}$ are reported. Porosity effects are taken into account using wave-scattering theory in a porous medium. The bulk modulus B_0 at atmospheric pressure for the nonporous matrix is 65 GPa, much smaller than $B(P)$ obtained at high pressures from lattice-parameter measurements. This discrepancy accrues from the large value of $(\partial B/\partial P)$. The comparatively small B_0 and large $(\partial B/\partial P)$ are due to vacant anion sites in this defect perovskite.

To obtain the pressure derivatives of the elastic stiffness, measurements have been made of the effects of hydrostatic pressure on the velocities of longitudinal and transverse ultrasonic waves propagated in polycrystalline ceramic specimens of the high- T_c superconductor $\text{YBa}_2\text{Cu}_3\text{O}_{7-x}$ (referred to as Y-Ba-Cu-O). The elastic stiffness constants C_{ijkl} quantify the second derivative of interatomic binding energy with respect to strain. The bulk modulus, in particular, is a prime parameter both experimentally and in theoretical calculations of the cohesive energy. Yet the actual value of the bulk modulus of Y-Ba-Cu-O is most uncertain. Previous ultrasonic wave-velocity measurements¹⁻⁴ give an adiabatic bulk modulus B_0 in the range of 40–50 GPa. However, x-ray determinations of lattice parameters under high pressure^{5,6} lead to much higher isothermal bulk modulus values which differ widely [180 GPa (Ref. 5) and 95 GPa (Ref. 6)]. The central aim here to reconcile these large discrepancies has been achieved by inclusion of the pressure dependence of the bulk modulus.

These ceramics are porous. To examine how the presence of pores influences the ultrasonic properties, measurements have been made on pressed pellets of Y-Ba-Cu-O, prepared by now-standard techniques, having widely different porosity n : sample Y1, $n=0.18$; sample Y2, $n=0.056$. Experimental techniques will be detailed elsewhere.⁷ Debye-Scherrer x-ray powder photography of sample Y1 gave lattice parameters $a=3.826 \pm 0.002$ Å, $b=3.888 \pm 0.002$ Å, and $c=11.677 \pm 0.003$ Å, and a theoretical density of 6338 kgm^{-3} . The correlation between oxygen content and c -axis lattice parameter⁸ suggests an oxygen composition of 6.8 per molecular unit (i.e., $x=0.2$). These small grained ceramics (grain size \ll ultrasonic wavelength) are treated as being isotropic bodies having two independent elastic stiffness moduli [C_{11} and C_{44} (=Lamé constant μ)]. Comparison be-

tween the results obtained for samples Y1 and Y2 (Table I) shows the important influence of the sample density and porosity on the elastic moduli. The presence of pores leads to reduction in the measured ultrasonic wave velocity. In view of the discrepancies between the published values of bulk modulus, it is important to establish the velocities which correspond to the nonporous matrix. This has been achieved by applying multiple-scattering theory developed⁹ for ultrasonic propagation in two-phase materials consisting of spherical inclusions in a matrix and extended¹⁰ self-consistently to a porous medium (when the scatterer is a void). The pores in these ceramics are irregularly shaped and have dimensions of about $5 \mu\text{m}$. Using the measured porosity and solving numerically the multiple-scattering equations in the low-frequency regime, we have calculated the ultrasonic wave-velocity values and hence the elastic stiffness moduli for the nonporous matrix quoted in Table I under YNP. The bulk modulus is increased by this correction for the effects of porosity but much less than is required to account for the bulk modulus differences found between the ultrasonic¹⁻⁴ and x-ray^{5,6} data. To find the reason for this difference, we need to take the pressure dependence of the bulk modulus into account.

The effects of hydrostatic pressure upon the velocity of longitudinal and shear 5-MHz ultrasonic waves propagated in sample Y1 (Fig. 1) are reproducible under pressure cycling and show no hysteresis. The ultrasonic wave velocity does not depend linearly upon pressure in the usual way but can be fitted by a parabolic curve. Hysteresis effects occur in sample Y2 on pressure and temperature cycling and seem to have the same origin.⁷ The hydrostatic pressure derivatives $(\partial C_{ij}/\partial P)_{P=0}$ of the elastic constants have been determined at room temperature in the limit as the pressure tends towards zero. To account for pressure induced changes in sample dimensions, the

TABLE I. Ultrasonic wave velocities, elastic constants, and their hydrostatic pressure derivatives for Y-Ba-Cu-O at 295 K. The data listed in the column labeled YNP correspond to the nonporous matrix and has been determined using multiple-scattering theory to take into account the effects of air-filled pores. The data listed in columns Y1^m and Y2^m also correspond to the nonporous matrix but has been determined from wave-propagation theory using Eqs. (1) and (2).

	Sample density (kg/m ³)	Ultrasonic wave velocity		Elastic constant		Bulk modulus B_0 (GPa)
		v_L (m/s)	v_S (m/s)	C_{11} (GPa)	$\mu (=C_{44})$ (GPa)	
Y1	5199	4067	2507	86.0	32.7	42.4
Y2	5985	4537	2893	123.0	50.1	56.4
YNP	6338	4780	3010	145	57.4	68.5
Y1 ^m					51	65.4
Y2 ^m					56.6	63.3

	Young's modulus E (GPa)	Poisson's ratio σ	Pressure derivative			Superconductivity transition temperature (K)
			$\partial C_{11}/\partial P$	$\partial C_{44}/\partial P$	$\partial B/\partial P$	
Y1	78.0	0.194	69.0	14.0	50	90
Y2	116.0	0.157	145	28	108	92
YNP	135	0.149				
Y1 ^m			108	17	85	
Y2 ^m						

natural velocity technique¹¹ was used. The hydrostatic pressure derivatives ($\partial C_{11}/\partial P$), ($\partial C_{44}/\partial P$), and ($\partial B/\partial P$) are very large (Table I).

These specimens take up silicone oil when immersed in it and subjected to pressure.⁷ In the case of sample Y1 98% of the pore volume had become filled with silicone oil after three pressure cycles. The pores must therefore be interconnected. An important problem to resolve is does the presence of oil-filled pores have a marked influence on the hydrostatic pressure derivatives of the elastic constants, even to the extent of being responsible for their very large values? To answer this, a theoretical treatment

of the wave propagation under pressure in an isotropic solid having a uniform distribution of pores has been developed. Full details of this wave propagation theory, of general applicability to porous ceramics, will be given elsewhere. An isotropic medium containing interconnected pores suffers a uniform compression under hydrostatic pressure and the porosity remains essentially unaltered. Since application of pressure saturates the pores with oil, ultrasonic velocity measurements under pressure provide the bulk B^n and shear μ^n moduli of the oil-saturated medium. The incremental moduli B^m and μ^m of the matrix under pressure have been shown to be given by

$$B = B^n + [n/(1-n)](3B^m + 4\mu^n)(B^n - B^w)/(3B^w + 4\mu^n), \quad (1)$$

$$\mu^m = \mu^n + [n/(1-n)][9B^n\mu^n + 8(\mu^n)^2 + 6\mu^m(B^n + 2\mu^n)]/(9B^n + 8\mu^n), \quad (2)$$

The bulk modulus B^w of the silicone oil has been measured as 1.0 GPa so its influence is small and independent of pressure. The bulk moduli B^m corresponding to the matrices of samples Y2 (including the hysteresis) and Y1 derived by inserting the experimental results into Eq. (1) are plotted in Fig. 2(a). Although the measured bulk moduli of the samples are quite different due to the different porosities, they are almost identical for the matrix. The shear modulus μ^m for sample Y1 determined from the experimental data using Eq. (2) is shown in Fig. 2(b).

The values of the bulk modulus B^m of the nonporous matrix determined both by the wave-propagation theory and from multiple-scattering theory are in good agreement, as expected in the low-pressure limit (Table I). Inspection of the ($\partial B/\partial P$) and ($\partial \mu/\partial P$) for the nonporous matrix (determined as the limiting gradient at zero pressure of the data in Fig. 2) shows that they retain large values which, therefore, cannot be a product of porosity.

The dependence of the ultrasonic wave velocity upon pressure has been measured only at comparatively low pressures (up to 0.15 GPa). The Murnaghan¹² equation of state has been used to determine the compression $V(P)/V_0$ at higher pressures for samples Y1 and Y2 [Fig. 3(a)]. Although $B_0(Y1) < B_0(Y2)$, the compressions are in the inverse order because the large value of ($\partial B/\partial P$) is the dominating factor. The effect of high pressure on unit-cell volume^{5,6} shows that Y-Ba-Cu-O does not comply with the predictions of the equation of state but has a nearly linear volume decrease with pressure [Fig. 3(a)] shown by the change in slope at about 7 GPa for the data presented as open circles which may well be a precursor to an orthorhombic-tetragonal transformation.⁶

The experimental value for ($\partial B/\partial P$) has been used in conjunction with the ultrasonically determined bulk modulus to estimate the bulk modulus $B(P)$ at pressure P [$= B_0 + (\partial B/\partial P)P$ to a first approximation] plotted in Fig. 3(b). It is now possible to compare directly the bulk

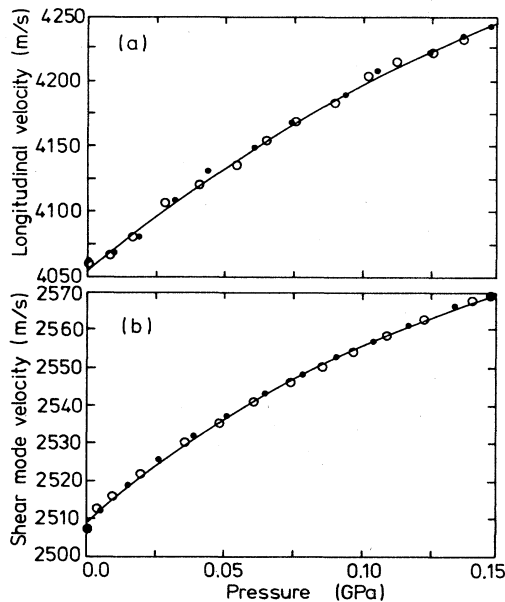


FIG. 1. The hydrostatic pressure dependence of the velocity of (a) longitudinal and (b) shear ultrasonic waves propagated in $\text{YBa}_2\text{Cu}_3\text{O}_{6.8}$ specimen Y1 at 295 K. The filled circles correspond to velocity measurements made with increasing pressure and the open circles to data obtained as the pressure was decreased. The solid line is the best fit to a parabolic curve.

modulus B_0 determined ultrasonically with that obtained from the x-ray lattice-parameter measurements. The reciprocal of the slope of the best-fit straight line to the compression data of Refs. 5 and 6 at the lower-pressure region gives the bulk modulus $B(P)$. Now the lattice parameters were measured at much higher pressures than

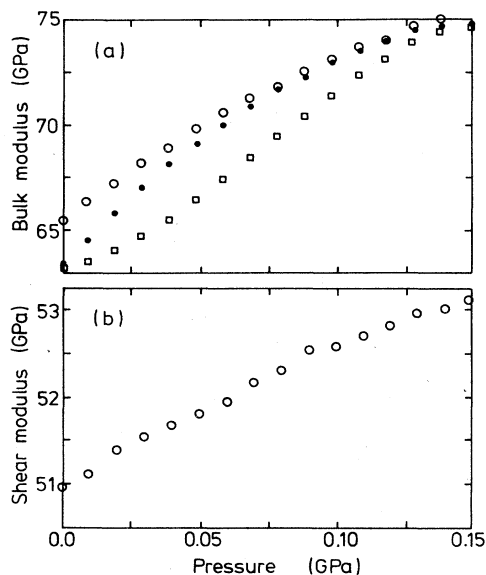


FIG. 2. The (a) bulk B^m and (b) shear μ^m moduli of the non-porous matrix of samples Y1 (open circles) and Y2 (squares, increasing pressure; filled circles, decreasing pressure) calculated from the experimental data using Eqs. (1) and (2), respectively.

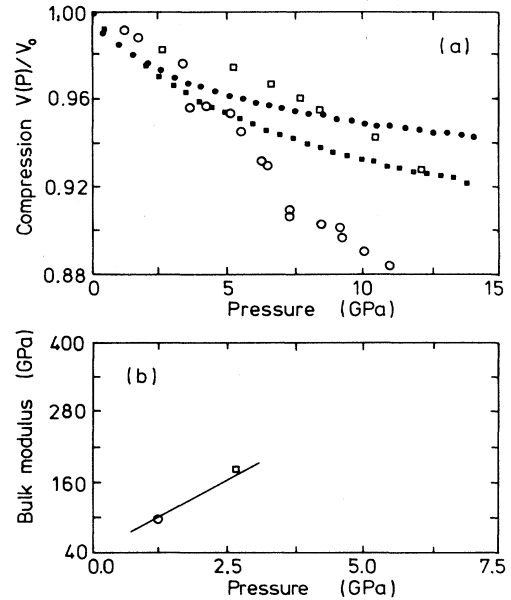


FIG. 3. (a) The compression of Y-Ba-Cu-O. The filled circles (Y1) and filled squares (Y2) correspond to compression calculated from the ultrasonic measurements of B_0 and $(\partial B/\partial P)_{P=0}$ using the Murnaghan equation of state. The other points correspond to compression determined from x-ray lattice-parameter measurements under pressure: open squares (Ref. 5), open circles (Ref. 6). (b) The pressure dependence of the bulk modulus $B(P)$ of Y-Ba-Cu-O. The solid line has been obtained using the ultrasonic data for B_0 and $(\partial B/\partial P)$. The square (Ref. 5) and circle (Ref. 6) correspond to values of $B(P)$ determined from the pressure dependence of the unit-cell volume. The data in Fig. 3(a) are not linear above about 2.5 GPa so the extrapolation is limited to that pressure.

those used in the ultrasonic experiments; the unit-cell volume is substantially reduced at these high pressures [Fig. 3(a)]. The bulk modulus reported by Ref. 5 and that obtained here from the data of Ref. 6 correspond to values for the material under high compression induced by high pressure. The $B(P)$ points obtained in each case fall close to the predicted $B(P)$ curve from the ultrasonic measurements of B_0 and $(\partial B/\partial P)$ [Fig. 3(b)]. Hence the results obtained by the two entirely different experiments are compatible; the large difference between B_0 and $B(P)$ arises simply from the enormous pressure derivative $(\partial B/\partial P)$. The lattice-parameter measurements are independent of the porosity. Hence the accord found between the two methods adds further support to the theoretical calculations which have established that neither the small B_0 nor its large pressure derivative result from porosity. Very large values of $(\partial C_{ij}/\partial P)$ and $(\partial B/\partial P)$ are an intrinsic material property of Y-Ba-Cu-O.

To explain why this considerably modified perovskite at atmospheric pressure has a small bulk modulus compared with standard perovskites ABO_3 and why the bulk modulus increases so much under applied pressure, recourse must be made to structural and interatomic binding considerations. Perovskites are ionically bound com-

pounds strongly resistant to compression: the bulk modulus of polycrystalline BaTiO₃ is 177 GPa. An important feature of Y-Ba-Cu-O is that it has a very low anion/cation ratio for a perovskitelike compound (being ~O₇ rather than O₉). In this defect perovskite the copper atoms are not surrounded by the complete octahedral oxygen cages characteristic of the standard ABO₃ perovskite structure but are in fourfold square-planar or fourfold square-pyramid coordination giving an open structure with a layered atomic arrangement. The influence of an ordered array of vacancies on the elastic properties of tetrahedrally bonded compounds has been examined¹³ in a series of vacancy compounds in which the number of empty cation sites progressively increases from zero: HgTe ($B=46.2$ GPa), Hg₅In₂□Te₈ ($B=38.9$ GPa), Hg₃In₂□Te₆ ($B=32$ GPa), HgIn₂□Te₄ ($B=29.9$ GPa).

As the density of vacant sites increases the bulk modulus reduces markedly. The large compressibility of vacancy compounds arises because the volume reduction induced by pressure is taken up around the empty sites. Vacancy compounds have enhanced values of $(\partial B/\partial P)$.¹⁴ Such compounds are easy to compress and rapid densification under pressure enhances the interatomic repulsion forces leading to a large $(\partial B/\partial P)$ and to the observed dramatic increase in the bulk modulus of Y-Ba-Cu-O under pressure towards a value more characteristic of perovskite compounds.

We are grateful to the Johnson Matthey Technology Center, Reading for financial support and encouragement. M. Cankurtaran is grateful to TÜBİTAK (Ankara) and to the Royal Society for support.

¹D. P. Almond, E. Lambson, G. A. Saunders, and Wang Hong, *J. Phys. F*, **17**, L221 (1987).

²Y. Horie, Y. Terashi, H. Fukuda, T. Fukami, and S. Mase, *Solid State Commun.* **64**, 501 (1987).

³M. Lang, T. Lechner, S. Riegel, F. Steglich, G. Weber, T. J. Kim, B. Lüthi, B. Wolf, H. Rietschel, and M. Wilhelm, *Z. Phys. B* **69**, 459 (1988).

⁴B. Wolf, T. J. Kim, H. Kühnberger, W. Palme, A. Krimmel, I. Xanthopoulos, W. Grill, B. Lüthi, and M. Schwarz, *Physica C* **153-155**, 284 (1988).

⁵W. H. Fietz, M. R. Dietrich, and J. Ecke, *Z. Phys. B* **69**, 17 (1987).

⁶N. V. Jaya, S. Natarajan, S. Natarajan, and G. V. S. Rao, *Solid State Commun.* **67**, 51 (1988).

⁷A. Al-Kheffaji, M. Cankurtaran, G. A. Saunders, D. P. Almond, E. F. Lambson, and R. C. J. Draper (unpublished).

⁸A. Ono, *Jpn. J. Appl. Phys.* **26**, L1223 (1987).

⁹P. C. Waterman and R. Truell, *J. Math. Phys.* **2**, 512 (1961).

¹⁰C. M. Sayers and R. L. Smith, *Ultrasonics* **20**, 201 (1982).

¹¹R. N. Thurston and K. Brugger, *Phys. Rev.* **133**, A1604 (1964).

¹²F. D. Murnaghan, *Proc. Nat. Acad. Sci. U.S.A.* **30**, 244 (1944).

¹³G. A. Saunders and T. Seddon, *J. Phys. Chem. Solids* **37**, 873 (1976).

¹⁴Tu Hailing, G. A. Saunders, and W. A. Lambson, *Phys. Rev. B* **26**, 5786 (1982).